Raman spectroscopy of human teeth using integrated optical spectrometers

N. Ismail,[1] L.-P. Choo-Smith,[2] K. Wörhoff,[1] A. Driessen,[1] A. C. Baclig,[3] P. J. Caspers,[3]
G. J. Puppels,[3] R. M. de Ridder,[1] and M. Pollnau[1]

[1] Integrated Optical Micro Systems Group, MESA+ Institute for Nanotechnology,
University of Twente, P.O. Box 217, 7500 AE Enschede, The Netherlands
[2] Institute for Biodiagnostics, National Research Council Canada, Winnipeg, Manitoba, Canada
[3] Center for Optical Diagnostics and Therapy, Department of Dermatology,
Erasmus-University Medical Center Rotterdam
n.ismail@ewi.utwente.nl

Abstract. *We have designed an arrayed-waveguide grating in silicon oxynitride technology for the detection of Raman signals from tooth enamel in the spectral region between 890 nm and 912 nm. The detected signals for both parallel and cross polarizations are used to distinguish between healthy and carious regions on the tooth surface of extracted human teeth. Our experimental results are in very good agreement with those achieved using conventional Raman spectrometers. Our results represent a step toward the realization of compact, hand-held, integrated spectrometers.*

Introduction

In the past decade researchers have shown that Raman spectroscopy can be used for the detection of dental caries [1, 2] giving complementary, and in some cases more accurate results than with conventional techniques such as visual inspection and OCT. In particular, the former method, which is exclusively based on the color perception of the human eye, lacks of accuracy when the detection has to be made on early dental caries. On the other hand, it has been demonstrated that polarized Raman spectroscopy gives can be used reliably for detecting dental caries even at an early stage.

Our aim is to realize low-cost, compact, hand-held devices for polarized Raman spectroscopy of teeth. The core element of our device is an arrayed-waveguide grating (AWG) [3] of which we show a schematic in Fig. 1.

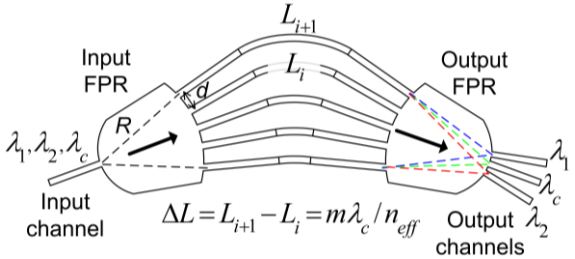

Fig. 1. Schematic layout of an arrayed waveguide grating (AWG), where FPR indicates the free propagation region, R is length of the FRP, d is the separation between the arrayed waveguides at the intersection with the FPR, λc indicates the central wavelength of the AWG, m is the order of the AWG, and L_i is the length of the i-th waveguide.

The working principle can be described as follows: light from an input channel waveguide is guided to a free-propagation region (FPR) where it diffracts in the horizontal direction and is coupled to an array of channel waveguides which are

arranged on a circle of radius R (grating line) equal to the length of the FPR. On this circle the arrayed waveguides are spaced by a center-to-center distance $d << R$. The arrayed waveguides have a linearly increasing length, and the length difference between adjacent waveguides is $\Delta L = m\lambda_c/n_{eff}$, where m is an integer, λ_c is the central wavelength of the AWG, and n_{eff} is the effective refractive index of the arrayed waveguides at the central wavelength. Light exiting from the array enters a second FPR where the output terminations of the arrayed waveguides are again arranged on a circle with radius R (as for the input FPR). The center of this circle coincides with the entrance facet of the central output channel of the AWG. With this arrangement, when light at wavelength λ_c is sent through the input channel, a circular wave front is generated at the output of the array, and the light is focused into the central output channel. For light at a different wavelength ($\lambda \neq \lambda_c$) the circular wave front generated at the output is tilted with respect to the one for λ_c, and the focal spot is located at a different spatial position. Output channels can be placed at different positions at the output of the second FPR to collect individual spectral components of the input signal. Compared to conventional spectrometers, the AWG presents smaller area (~ cm^2) and can be integrated on a chip. A potential disadvantage, the limited free spectral range (FSR) achievable for a given device size, can be overcome by a technology platform providing larger refractive index contrast, e.g. silicon photonics, or by accepting spectrally folded, yet non-overlapping peaks, as discussed in [4].

Detection of early dental caries by polarized Raman spectroscopy

The method relies on measuring the Raman signals from tooth enamel within the so-called fingerprint region, which extends from approximately 375 cm^{-1} to 1175 cm^{-1}. In this spectral region the strongest band is the symmetric P-O stretching vibration of the phosphate ions $(PO_4)^{3-}$ located near 959 cm^{-1}, which arises from hydroxyapatite crystals of tooth enamel. Information on the state of the disease is provided by the ratio of the intensities of two orthogonal polarization states (perpendicular and parallel to the polarization of the excitation laser) of the 959 cm^{-1} hydroxyapatite peak. Their intensity ratio is referred to as the depolarization ratio, $\rho_{959} = I_{959}(\perp) / I_{959}(\parallel)$. In sound enamel the hydroxyapatite signal is highly polarized in the direction parallel to that of the excitation laser, and the value of the depolarization ratio is approximately $\rho_{959} = 0.10 \pm 0.04$ [2]. As the carious lesion develops, there is a gradual structural modification of the tooth enamel, which also affects its optical properties, causing ρ_{959} to increase to ~0.4 ± 0.12 [2].

The AWG was designed to be used with an excitation wavelength of 830 nm (as in Ref. 2). For this excitation wavelength the hydroxyapatite peak is positioned at ~901 nm. To resolve the peak the AWG was designed to have a central wavelength of 901 nm, a FSR of ~22 nm between 890 and 912 nm, and a resolution of 0.2 nm. The AWG was fabricated using single-mode silicon oxynitride [5] channel waveguides with with 2.2 μm width and 0.52 μm height. The waveguide core and cladding refractive indices were 1.509 and 1.445 at 830 nm, respectively. The AWG was designed to have a working order of m = 41 to avoid overlap (at higher imaging orders) between the excitation wavelength and the hydroxyapatite peak. Additional details on the design and characterization can be found in [4].

Polarized Raman measurements using the AWG

To perform polarized Raman measurements using the AWG we used the setup shown in Fig. 2. Light from a linearly polarized, tunable Ti:Sapphire laser at 830 nm was sent through a polarization beam splitter (PBS) oriented parallel to the laser polarization. A half-wave plate, initially with one of its optical axes parallel to the laser polarization, was placed after the PBS. The laser light exiting the λ/2 plate, after passing through a laser-line filter (Semrock LL01-830-12.5), was reflected from a dichroic mirror (Semrock LPD01-830RS-25) and focused onto the sample (extracted human tooth) with a ×40 microscope objective having numerical aperture NA = 0.65. The light backscattered from the sample was then collected by the same optics. The Rayleigh-scattered component was again reflected (rejected) by the dichroic mirror while the Raman-scattered wavelengths were transmitted. An edge filter (Semrock LP02-830RS-25) and an additional red-glass filter (RG 850) were used to further suppress residual reflected and Rayleigh-scattered light at the laser wavelength. At this point we positioned a second PBS with the same orientation as the first, and a ×50 (NA = 0.85) microscope objective to focused the light onto the input channel of the integrated AWG spectrometer. The spectroscopic measurement was performed imaging the output channels of the AWG onto an electron-multiplying charge-coupled device (Andor iXonEM DV887ECS-BV, EMCCD) through a camera lens (JML f0.95 50 mm). In order to perform the measurements for perpendicular polarization, the λ/2 plate was simply rotated by 45°, so that the polarization of the excitation laser was rotated by 90°.

Since in both, parallel and cross-polarization measurements, the light entering the AWG was always horizontally polarized (TE polarization with respect to the input waveguide) there was no need to calibrate for the polarization dependence of the AWG.

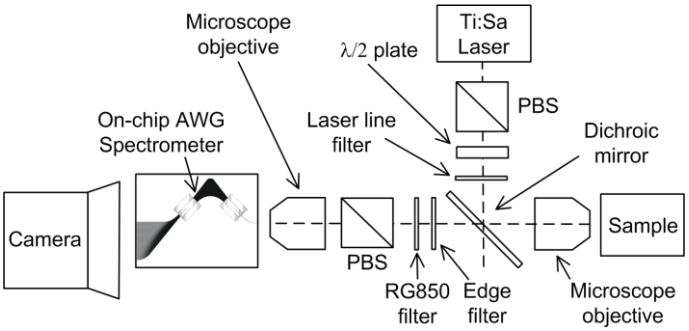

Fig. 2. Schematic diagram of the setup used for the polarized Raman experiments.

The measurements were performed on two extracted human tooth samples presenting clinical white spot lesions as early dental caries. The locations on the tooth surface on which to perform the measurements were chosen based upon previous visual examination by a dental clinician. We used an excitation wavelength of 830 nm with 200 mW of incident power on the tooth surface. Measurements were carried out on three healthy and three carious regions. The Raman signal from these regions was strong and clearly visible with integration times as short as 10 s. In Fig. 3 we show representative spectra measured with 80 s integration time and 10 accumulations. The trends of the spectral intensities at 959 cm^{-1} are consistent with polarized Raman spectra acquired using a conventional Raman spectrometer (LabRamHR, Horiba Jobin Yvon) from the same tooth samples (see inset). In each of the six regions, we calculate the

depolarization ratio and obtain an average value of $\rho_{959} = 0.16 \pm 0.047$ for the sound regions and $\rho_{959} = 0.41 \pm 0.01$ for the carious regions. These numbers are close to the values reported in the literature [2]. The depolarization ratios are calculated using the peak intensities at 959 cm^{-1} relative to the adjacent baseline. The sharp peak at ~1050 cm^{-1} is attributed to the laser line imaged at higher order (m = 45) and was verified to be independent of the nature of investigated sample [4].

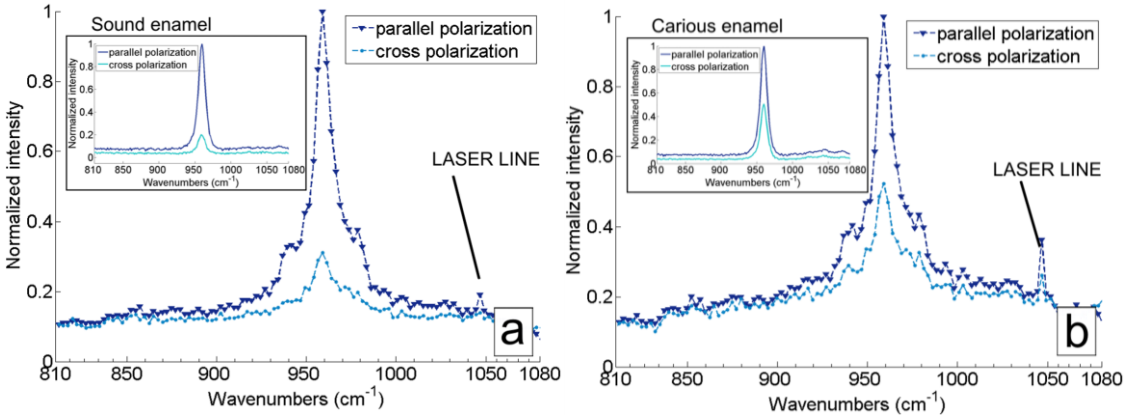

Fig. 3. Raman spectra of (a) sound and (b) carious tooth enamel for both, parallel (triangles) and cross (dots) polarizations acquired with the AWG. The insets show spectra acquired with a conventional Raman spectrometer.

Conclusions

We have designed and fabricated an AWG spectrometer to be used in polarized Raman spectroscopy of human teeth. Our measurement results, which are comparable with the ones found in the literature for both, sound and carious regions of tooth enamel, demonstrate the feasibility of our approach.

Acknowledgment

This work was supported in the Innovative Research Program (IOP) Photonic Devices funded by the Dutch Ministry of Economic Affairs. The authors thank C. Otto from the Medical Cell BioPhysics (MCBP) group of the University of Twente for providing the EMCCD array.

References

[1] W. Hill and V. Petrou, "Caries Detection by Diode Laser Raman Spectroscopy," Applied Spectroscopy, vol. 54, pp. 795-799, 2000.

[2] A. C.-T. Ko, L.-P. i. Choo-Smith, M. Hewko, M. G. Sowa, C. C. S. Dong, and B. Cleghorn, "Detection of early dental caries using polarized Raman spectroscopy," Optics Express, vol. 14, pp. 203-215, 2006.

[3] M. K. Smit, "New focusing and dispersive planar component based on an optical phased array," Electronics Letters, vol. 24, pp. 87-88, 1988.

[4] N. Ismail, L.-P. Choo-Smith, K. Wörhoff, A. Driessen, A. C. Baclig, P. J. Caspers, G. J. Puppels, R. M. de Ridder, and M. Pollnau1, "Raman spectroscopy with an integrated arrayed-waveguide grating," Optics Letters, 2011.

[5] K. Wörhoff, C. G. H. Roeloffzen, R. M. d. Ridder, A. Driessen, and P. V. Lambeck, "Design and application of compact and highly tolerant polarization independent waveguides," Journal of Lightwave Technology, vol. 25, pp. 1276-1283, 2007.